Scientific Research Publishing

Open Journal of Inorganic Non-metallic Materials, 2020, 10, 1-14
https://www.scirp.org/journal/ojinm
ISSN Online: 2164-6805
ISSN Print: 2164-6791

Synthesis, Characterization and Biological Activity of Sodium Barbitone-Group-VIII Metals (viz. Ni(II), Pd(II) and Pt(II)) Complexes

Fatma S. M. Hassan*, Wafaa S. Kuran, Asmaa A. Ibrahim, Farouk A. Adam

Chemistry Department, Faculty of Science, Aswan University, Aswan, Egypt
Email: *Fatma_smh@yahoo.com

How to cite this paper: Hassan, F.S.M., Kuran, W.S., Ibrahim, A.A. and Adam, F.A. (2020) Synthesis, Characterization and Biological Activity of Sodium Barbitone-Group-VIII Metals (viz. Ni(II), Pd(II) and Pt(II)) Complexes. *Open Journal of Inorganic Non-metallic Materials*, **10**, 1-14.
https://doi.org/10.4236/ojinm.2020.101001

Received: January 2, 2020
Accepted: January 28, 2020
Published: January 31, 2020

Abstract

This work aims to characterize, synthesize and evaluate the biological activity of sodium barbitone and their metal chelates Ni(II), Pd(II) and Pt(II). The new synthesized metal chelates are investigated by elemental analysis, IR, mass spectra, thermal analysis and biological activity. Square planer structure of the prepared complexes obtained from the result of analysis. The antibacterial and antifungal of sodium barbitone ligand and its conforming metal chelates were screened against bacterial species Gram positive (*Staphylococcus aureus*), Gram negative bacteria (*Escherichia coli*) and fungi *Aspergillus flavus* and *Candida albicans* fungi. Ampicillin and amphotericin were used as references for antibacterial and antifungal studies. The activity data show that the platinum group metals chelates have activity data show that some of the platinum group metals (viz. Pt(II) and Pd(II)) chelates have a promising biological activity comparing to sodium barbitone parent free ligand against bacterial and fungal species.

Keywords

Sodium Barbitone, Group VIII Metals, Transition Metals Complexes, Spectroscopic Analyses, Thermal Analysis, Biological Activity

1. Introduction

Sodium barbitone 5,5-diethyl barbiturate derived from barbituric acid belongs to the family of 2,4-pyrimidione, is prepared by the neutralization of an aqueous solution of lactam with sodium hydroxide and then precipitating the salt by the addition of alcohol (Scheme 1). Sodium barbitone plays an important role in pharmaceutical applications it is a category of drugs that have varied applica-

tions such as sedatives, hypnotics and anticonvulsants under an assortment of conditions and is also employed for anesthesia [1] [2].

Sodium barbital solutions have also been used as pH buffers for biological research, e.g., in immunoelectrophoresis or in fixative solutions [3] [4]. As barbital is a controlled substance, barbital-based buffers have largely been replaced by other substances [5].

The coordination chemistry of organotransition-metal complexes which have biologically active ligands has attracted tremendous interest over the years. The study of this complexes enable us understanding the role of these ligands in biological systems, in many biological systems compounds which containing pyrimidine ring play an important role, where they exist in nucleic acids, several vitamins, coenzymes and antibiotics [6] [7]. The nucleic acid is related to antimetabolites used in anticarcinogenic chemotherapy [8]. In recent years, the metal complexes of pyrimidine widely taught owing to their great variety of biological activity ranging from antimalarial, antibacterial, antitumoral, antiviral activities etc. [9]-[15].

The manufacture of plastics and pharmaceuticals products used barbituric acid. Phenobarbital (5-ethyl-5-phenylbarbituric acid) is the drug used most commonly for convulsive disorders and is the drug of choice for infants and young children [16].

Barbiturates have a wide range of medicinal applications and have ability to coordinate with transition metals through one or both deprotonated nitrogen and carbonyl oxygen atoms, synthesis of their metal complexes has attracted our attention to synthesize and characterize barbitone complexes with nickel and some of the platinum group metals [Pd(II) and Pt(II)].

2. Experimental

2.1. Reagents and Materials

In this study, the chemicals used are of highest purity available, it included sodium barbitone, $NiCl_2 \cdot 6H_2O$ and $Pd(C_4H_6O_4)$; which are purchased from Aldrich and K_2PtCl_4; is a gift from Professor Paul G. Pringle of Bristol University, UK. All are used without further purification. The solvents such as absolute ethanol, methanol, acetone and DMF were purchased from Sigma and are spectroscopic pure. De-ionized water was collected from all glass equipment and used in all preparations.

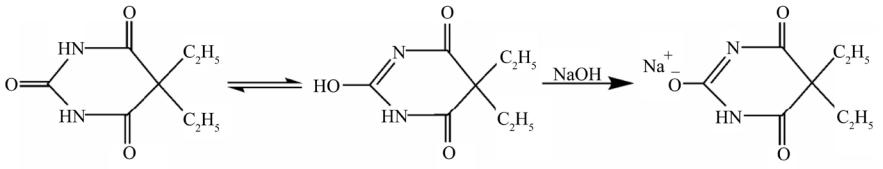

Scheme 1. Synthesis of Na[Hdebarb].

2.2. Instrumentation

Weights measurement was performed by using Sensitive analytical balance [0.0001 g, SCALTEC (Germany)]. Stirring and heating were performed by using magnetic stirrer theromostated hot plate (VELPEurope). Automatic pipette is used to take very small volumes of solvents. Melting points were detected in capillary tube using (Gallen Kamp) and elemental microanalysis measurements were performed in the National Research Center Cairo for C, H and N.

The infrared spectra were measured using a Perkin Elmer FTIR type in the wave number region 4000 - 400 cm^{-1}. The electron impact (EI) mass spectra MS at 70 ev of the tested compounds has been done using Shimadzu GC-MS-Qp 1000 PX quadruple mass spectrometer. Thermal analysis (TGA and DTG) were carried out in dynamic nitrogen atmosphere (20 m/min^{-1}) with heating rate of 10˚C min^{-1} using conventional thermal analyzer (Shimadzu system of DTA-50 and 30 series TG-50). The molar magnetic susceptibility was measured on powdered samples using the Faraday method. The diamagnetic corrections were made by Pascal's constant and $Hg[Co(SCN)_4]$ was used as a calibrant.

2.3. Methods

2.3.1. Synthesis of $[Ni(C_8H_{11}N_2O_3)Cl{\cdot}H_2O]8H_2O$

Sodium 5,5-diethyl barbiturate ligand (2.47 g, 0.011 mol) was dissolved in least amount of bidistilled water, then added to $NiCl_2{\cdot}6H_2O$ (0.95 g, 0.003 mol). The total volume was completed to 50 ml using bidistilled water. The reaction mixture was stirred for 60 minutes, a pale green precipitate was appeared, filtered off and washed thoroughly with methanol several times. It was recrystallized from DMF/ethanol mixture, dried in desiccator using $CaCl_2$. Yield 76.71%, (M.P 310˚C - 312˚C).

2.3.2. Synthesis of $[Pd(C_8H_{11}N_2O_3)(ACO){\cdot}H_2O]4H_2O$

Sodium 5,5-diethyl barbiturate ligand (0.618 g, 0.003 mol) was dissolved in least amount of distilled water, then added to $Pd(CH_3COO^-)_2$ (0.224 g, 0.001 mol) solution and in acetone. The volume of reaction mixture was completed to 30ml stirred at room temperature for 60 minutes, dark oily precipitate was resulted. It was filtered off, washed thoroughly with methanol, recrystallized from DMF/ethanol mixture, dried in desiccator containing $CaCl_2$. Yield 77%, (decomposed at 308˚C).

2.3.3. Synthesis of $[Pt(C_8H_{11}N_2O_3)CL{\cdot}H_2O]2H_2O$

Sodium 5,5-diethyl barbiturate ligand (0.618 g, 0.003 mol) was dissolved in least amount of distilled water, then it was added to $K_2Pt\ Cl_4$ (0.415 g, 0.001 mol). The volume of reaction mixture solution was completed to 15 ml with distilled water. It was stirred at room temperature for 24 hours, an oily green precipitate was appeared it was filtered off and washed thoroughly with distilled water several times, recrystallized from DMF/ethanol mixture, dried in desiccator containing $CaCl_2$. Yield 78%, (decomposed at 320˚C).

2.4. Biological Activity

Modified Kirby-Bauer disc diffusion method [17], has been used to determine the antimicrobial activity of the tested samples. Disc diffusion method for yeast developed by National Committee for VlinicalLaboratory Standards using approved standard method (M44-P). Plates inoculated with filamentous fungi as *asprgillus flavus* at 25˚C for 48 hours; Gram (+) bacteria as *Staphylococcus aureus*; Gram (-) bacteria a *Escherichia coli*, they were incubated at 35˚C - 37˚C for 24 - 28 hours and yeast as *Candida albicans* incubated at 30˚C for 24 - 28 hours, then the diameters of the inhibition zones were measured in millimeters withslipping calipers of the National Committee for Vlinical Laboratory Standards.

3. Results and Discussion

3.1. Physical Properties and Elemental Analysis

The elemental analyses data of the given group VIII metals metal chelates considerable with the theoretical values within the limit of experimental mistake; as shown in Table 1.

3.2. FT-IR Spectroscopy

The FT-IR data of the free ligand and its corresponding metal chelates are examined and the results are presented in Table 2.

Table 1. Properties of new complexes of molar ratio (1:1) of Ni(II), Pd(II) and Pt(II).

Compound	Mol.Wt	Color	M.P ˚C	%C Calc. (found)	%H Calc. (found)	N% Calc. (found)	μ_{eff}
$[Ni(C_8H_{11}N_2O_3)Cl{\cdot}H_2O]8H_2O$	439.49	Pale green	310 - 312	21.86 (21.79)	6.65 (6.64)	6.37 (6.30)	0.0
$[Pd(C_8H_{11}N_2O_3)(ACO){\cdot}H_2O]4H_2O$	438.71	Dark oily	308	27.37 (27.43)	5.51 (5.54)	6.38 (6.5)	0.0
$[Pt(C_8H_{11}N_2O_3)CL{\cdot}H_2O]2H_2O$	467.78	Oily green	320	20.54 (20.55)	3.66 (3.65)	5.98 (5.93)	0.0

μ_{eff}: effective magnetic moment.

Table 2. Infrared spectrum data of sodium barbitone and its metal chelates (band maxima in Cm^{-1}).

Compound	υ(C=O) amide(I) (N-C=O)	υ(NH) amide	υ(C=O) carbonyl	υ(C-O)	υ(=C-O-)	υOH	υ(M-Cl)	υ(M-O)	υ ring	υ(M-N)
Sodium barbitone ($C_8H_{11}N_2O_3Na$)	2467w	3182s	1667s	1461s	1164m	_____	_____	_____	843s	_____
$[Ni(C_8H_{11}N_2O_3)Cl{\cdot}H_2O]8H_2O$ (1)	_____	3213b	1678s	1400m	1165w	3427sb	471w	618s	872m	618.30sb
$[Pd(C_8H_{11}N_2O_3)(ACO){\cdot}H_2O]4H_2O$ (2)	2354w	3234b	1637s 1681s	1405m	1182w	3545sb	_____	438w 549m	770m	549.35s
$[Pt(C_8H_{11}N_2O_3)CL{\cdot}H_2O]2H_2O$ (3)	_____	3242b	1637s 1687s	1408m	1183w	3458mb	474 w	471.94w 549 m	772m	549.246m

Band property: s = strong, m = medium, w = weak.

The IR data of metal chelates complexes are given in **Table 2**. The IR display various sharp bands in the mid infrared region, clearly indicating the presence of barbital [18]. The strong and broad absorptions bands at 34,583,545 and 3427 in complexes 1, 2 and 3 respectively are due to of lattice water [19]. The insignificant shifts of υ NH in complexes 1-3 as compared to ligand (3182 cm^{-1}) are detected at 3242 cm^{-1} (Ni), 3213 cm^{-1} (Pd), and 3234 cm^{-1} (Pt), respectively, probably due to formation of hydrogen bonds. The frequency range of 1637 - 1687 cm^{-1} have mastery over very strong IR and Raman bands arising from carbonyls. The change observed for carbonyl vibrations υ C=O which in position 4, 6 and υ C-O which in position 2 **Figure 1**, diagnostic for its participation in coordination. The υ C=O in complexes 1 and 3 are observed as two distinct absorptions from 1637 to 1687 cm^{-1}, while in complex 2 absorptions bands at 1637 and 1681 cm^{-1}. The υ C=O in position 4, 6 do not correlate predictably with coordination modes of this group. This may be due to the presence of strong intra or intermolecular hydrogen bonding interactions [20], which affect the carbonyl bands, shifting them to lower frequencies. The υ C-O in position 2 also shifted to lower frequencies (14,081,405, and 1400 cm^{-1} for complexes 1, 2, and 3, respectively) compared to that of the ligand (1461 cm^{-1}). This indicates that the barbital anions are coordinated to metal via the carbonyl oxygen O which in position 2. This is further confirmed by the appearance of a medium intensity band at 438 - 618 cm^{-1} in spectra of the complexes, assigned to stretch of M-O [21] **Table 2**. The comparative studies of FTIR for the free ligand and its corresponding metal chelates prove the proposed structure of the complexes which is shown in **Figure 1**.

3.3. Mass Spectra of Sodium Barbitone Metal Chelates

The electron impact mass spectra (EI-MS) of the newly prepared complexes are recorded at 70 ev and investigated. The mass spectrum for $[Ni(C_8H_{11}N_2O_3)Cl{\cdot}H_2O]8H_2O$ was recorded and investigated **Figure 2**.

3.3.1. Mass Spectrum of $[Ni(C_8H_{11}N_2O_3)Cl{\cdot}H_2O]8H_2O$

The electron ionization (EI-MS) mass spectrum for $[Ni(C_8H_{11}N_2O_3)Cl{\cdot}H_2O]8H_2O$ display a signal at m/z = 439.85 (mole mass = 439.48, RI = 0.8%) this signal may be referred to the appearance of main molecular formulae ion. Through three parallel pathways this fragment is broken which are presented in **Scheme 2**.

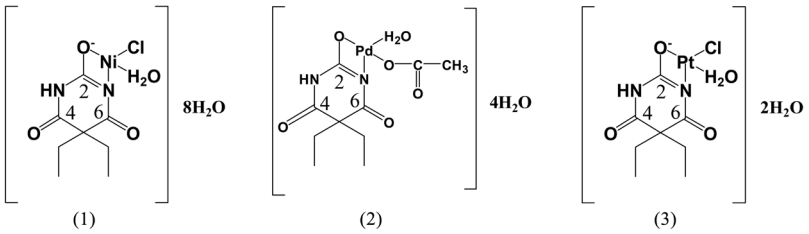

Figure 1. Proposed structure of the complexes Ni(II), Pd(II) and Pt(II).

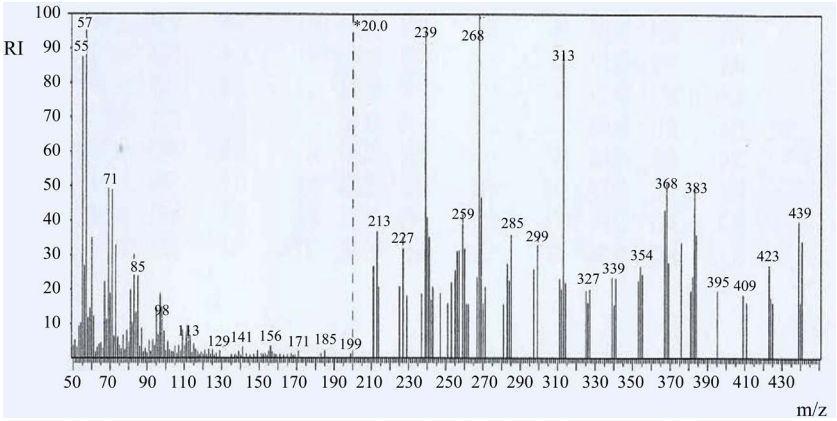

Figure 2. Mass Spectrum of $[Ni(C_8H_{11}N_2O_3)Cl{\cdot}H_2O]8H_2O$.

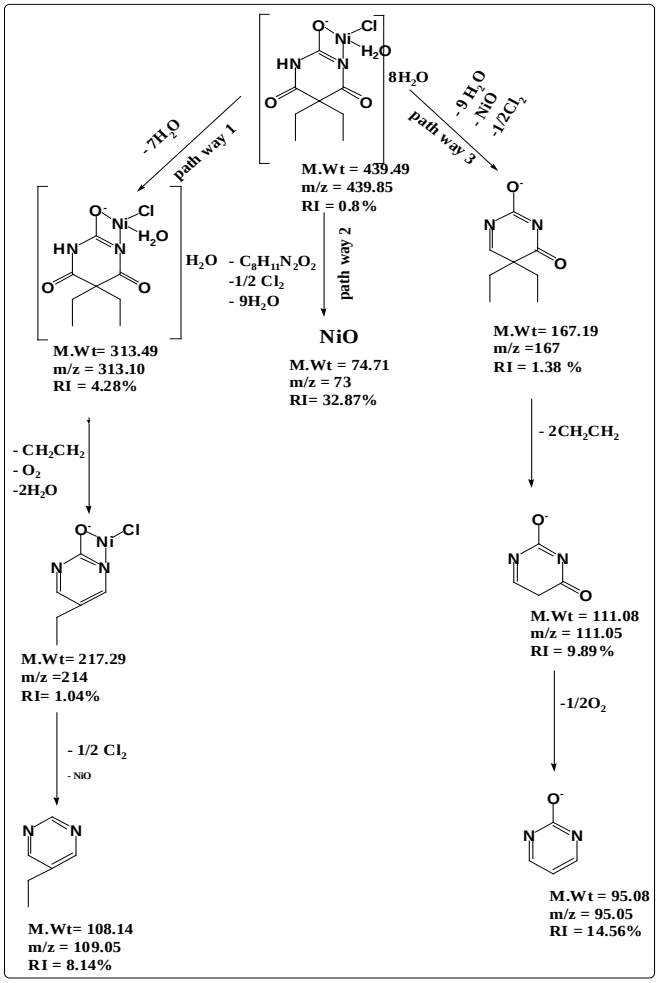

Scheme 2. The mass fragmentation pathways of Ni(II) chelate with sodium barbitone.

Pathway (1) display fragment ion at m/z = 313.10 (mole mass = 313.49, RI = 4.28%) due to the rupture of seven molecule of water after that the signal at m/z = 214 (mole mass = 217.29, RI = 1.04%) due to the loss of (CH_2CH_2, O_2 and $2H_2O$). The signal at m/z = 109.05 (mole mass = 108.14, RI = 8.14%) due to the

rupture of $1/2O_2$ and NiO. Pathway (2) shows fragment ions at m/z = 73 (mole mass = 74.71, RI = 32.87%) attributed to the loss of ($C_8H_{11}N_2O_2$, 1/2 Cl_2 and $9H_2O$). The third pathway shows fragment ions at m/z = 167, 111.05 and 95.05 (RI = 1.38%, 9.89% and 14.56%, respectively.); these fragments may be attributed to the loss of $9H_2O$, NiO and $1/2Cl_2$ followed by the loss of two molecules of Ethene followed by the loss of $1/2O_2$.

3.3.2. Mass Spectrum of [Pd ($C_8H_{11}N_2O_3$)(CH_3COO)H_2O]$4H_2O$

The mass fragmentation of [Pd ($C_8H_{11}N_2O_3$)(CH_3COO)H_2O]$4H_2O$ chelate consists of three principal pathways presented in Scheme 3. Pathway 1 display a signal at m/z = 348.20 (RI = 0.25%) due to loss of $5H_2O$ after that loss CH_3COOH and PdO at m/z = 167.10 (mole mass = 168.19, RI = 5.41%) followed by loss of molecule of oxygen and two molecule of ethen at m/z = 85.15 (mole mass = 84.12, RI = 36.34%). In pathway (2), the fragment at m/z = 288.10 (mole mass = 288.58, RI = 1.24%) refers to the loss of $5H_2O$ and acetic acide. This step is followed by loss of PdO, O_2 and ethen with m/z = 111.15 (mole mass = 110.88, RI = 14.01%) then loss molecule of CH_2CH_2 at m/z = 85.15 (mole mass = 84.12, RI = 36.34%). Pathway (3) shows signal at m/z = 185.15 (mole mass = 184.95, RI = 2.97%) as loss of five water molecules and palladium acetate followed by loss of $C_4H_4N_2O_3$ at m/z = 57.10 (mole mass = 56.108, RI = 100%).

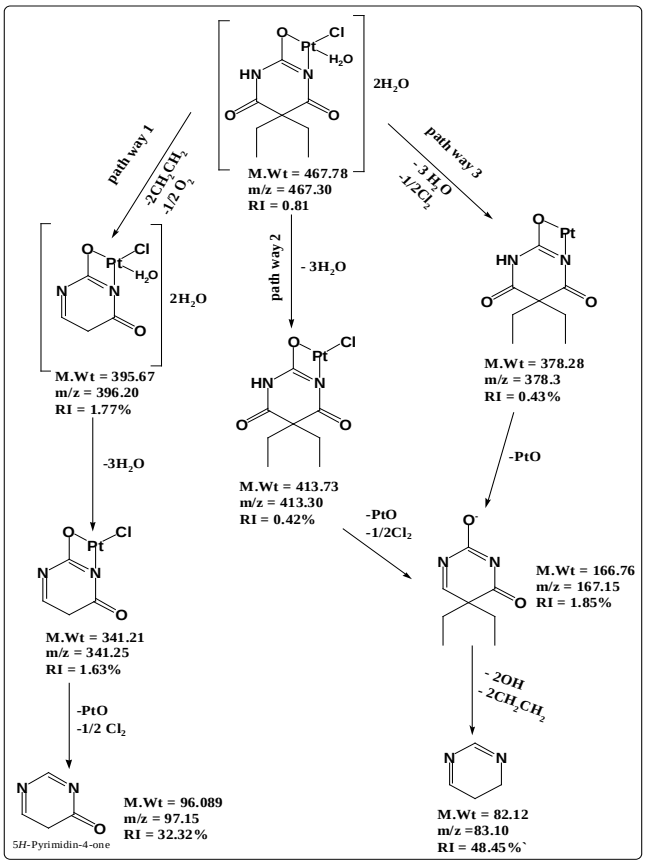

Scheme 3. The mass fragmentation pathways of Pt(II) chelate with sodium barbitone.

3.3.3. Mass Spectrum of [Pt ($C_8H_{11}N_2O_3$)Cl·H_2O]2H_2O

The mass fragmentation of [Pt($C_8H_{11}N_2O_3$)Cl·H_2O]2H_2O chelate after ionization of neutral molecule at 70 eV consists of three principal pathways as rationalized in Scheme 4. The signal that appears at 467.30 (RI = 0.81%) may be impute to the apparition of the essential molecular ion. This molecular ion is due to loss of two molecule of ethane and 1/2 O_2 appearance of the signal at m/z = 396.20 (RI = 1.77%) followed by the loss of three water molecules appearance of signal at m/z = 341.25 (mole mass = 341.21, RI = 1.63%) after that loss of PtO and 1/2 Cl_2 m/z = 97.15 (mole mass = 96.089, RI = 32.32%). Pathway II display a signal at m/z = 413.30 (mole mass = 41373, RI = 0.42%) due to the loss of 3H_2O, followed by elimination of PtO and 1/2Cl_2 with a signal at m/z = 167.15 (mole mass = 166.76, RI = 1.85%), followed by the loss of 2OH and two molecule of ethane m/z = 83.10 (mole mass = 82.12, RI = 48.45%). Pathway III display a signal at m/z = 378.3, 167.15 and 83.10 (RI = 0.43%, 1.85% and 48.45%) due to loss of 1/2Cl_2 and three coordinated water molecules followed by the loss of PtO after that loss of 2OH and two molecule of ethane.

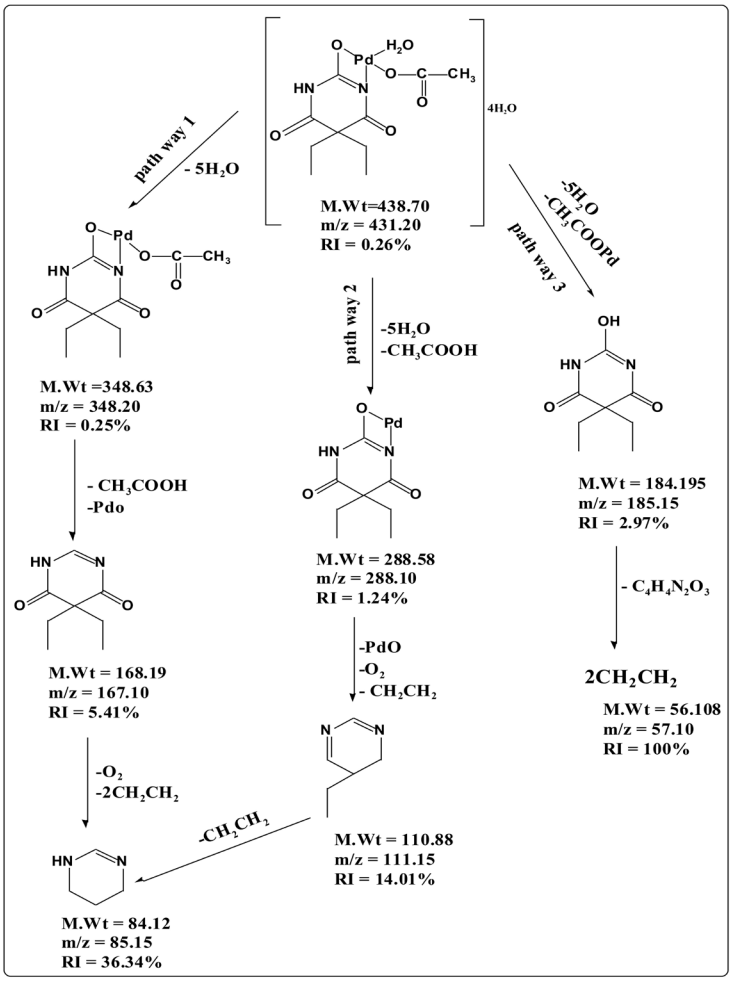

Scheme 4. The mass fragmentation pathways of Pd (II) chelate with sodium barbitone.

3.4. Magnetic Moments and Electronic Spectral Data of Metals Complexes

The UV-Visible spectrum of Ni(II) complex showed peaks at 260 nm (38,461 cm^{-1}), 305 nm (32,786 cm^{-1}) and at 546 nm (18,315 cm^{-1}) assigned to $\pi \rightarrow \pi^*$, LMCT and $^1A1g \rightarrow {}^1A2g$ respectively, then confirmed the square-planner environment around nickel (II) ion [22] [23]. The electronic spectrum for the complexes of Pd (II) complex showed the absorption peaks at 246 nm (40,650 cm^{-1}) (901 $molar^{-1}$ cm^{-1}) 305 nm (32,786 cm^{-1}) and 376 nm (26,595 cm^{-1}). These transitions belonged to intra-ligand charge transfer, LMCT and $^1A1g \rightarrow {}^1A2g$ of $4d^8$ configuration of Pd(II) ion [24]. The electronic spectrum for the Pt(II) complex exhibited the absorption peaks at 258 nm (38,759 cm^{-1}), 305 nm (32,786 cm^{-1}) and 540 nm (18,518 cm^{-1}) indicating the ($\pi \rightarrow \pi^*$) of chromophores; -C=N-while the second peak is attributed to MLCT respectively [24]. Ni (II), Pd(II) and Pt(II) were in well-agreement of electronic spectra to confirm their square-planner symmetry as in Table 3.

3.5. Thermal Analyses

The TGA thermal analysis data of the synthesized metal chelates are tabulated in Table 4. The thermal decomposition of $[Pt(C_8H_{11}N_2O_3)Cl{\cdot}H_2O]2H_2O$ metal chelate as an example occurs through three steps. The first step occurs at temperature 36.56˚C - 279.23˚C with mass loss of 7.7% (calcd.11.5%). This step may be assigned to the loss of three molecules of water. The second step occurs at temperature range of 279.23˚C - 350.62˚C this range may correspond to the removal of $1/2Cl_2$ and $1/2O_2$ with observed mass loss of 7.097% (calcd. 12.4%). The third step occurs at temperature 350.62˚C - 601.43˚C with mass loss of 37.7% (calcd 41.73%) this step due to the separation of $C_8H_{11}N_2O$. The total practical mass loss may be 52.59% (calcd. 55.55%). The remainder product may be PtO with practical mass 47.41% (calcd. 45.13%).

The second metal chelate $[Pd(C_8H_{11}N_2O_3)(CH_3COO)H_2O]4H_2O$ decomposed through two steps. The first step occurs at range 8.80˚C - 250.73˚C with mass loss of 3.489% (calcd. 4.1%). This mass loss may be attributed to the removal of one coordinated water molecule. The second step occurs at range 251.30˚C - 601.74˚C with mass loss of 66.14% (calcd 71.14) due to the separation of ($4H_2O$, CH_3COOH and $C_8H_{11}N_2O_2$) leaving PdO as remainder product with practical mass 30.347% (calcd. 27.98%). Three decomposition steps appear in the thermal analysis $[Ni(C_8H_{11}N_2O_3)Cl{\cdot}H_2O]8H_2O$ complex. The first one may correspond to the loss of nine molecule of water with mass loss of 20.8% (calcd. 36.9%). The second occurs at 212.76˚C - 332.96˚C with a mass loss of 11.8% (calcd. 15.9%), which may be attributed to the loss of ethene and $1/2O_2$. The third step of decomposition (332.96˚C - 501.77˚C) may be assigned to the loss of CH_3Cl, NH_3 and $1/2O_2$ leaving NiO + Penta-2,4-diynenitrile as a remainder product with practical mass 31.117% (calcd. 36.03%). To determine the value of the residue, we divide the molecular weight of the residue by the molecular weight of the

whole complex for example in the case of [Pt ($C_8H_{11}N_2O_3$)Cl·H_2O]2H_2O metal chelate (mo.t = 467.7768) the remainder product PtO with molecular weight 211.09 to detect the value of residue we perform the following calculation ((211.09/467.7768) × 100) = 45.13%.

4. Biological Activity

The comparison of the biological activity of the sodium barbitone and its corresponding metal chelates with the standards (ampicillin and amphotericin for antimicrobial and antifungal respectively) towards different organisms was described. The data are recorded in Table 5 and shown in Figure 3. The free ligand and its metal chelates were screened against C.albicans and A.flavas (fungi), S.aureus (G^+) and E.coli (G^-) to assess their potential antimicrobial agent.

Table 3. Electronic spectral data and magnetic moments of metals complexes. (MLCT = Metal-ligand charge transfer).

Complex	Observed bands (λmax/nm)/(ν max/cm^{-1})	Assignments	Symmetry	μ_{eff} B.M
[Ni($C_8H_{11}N_2O_3$)Cl·H_2O]8H_2O	260/38,461 305/32,786 546/18,315	π → π* LMCT 1A1g → 1B1g	Square planner	0.0
[Pd($C_8H_{11}N_2O_3$)(CH_3COO)H_2O]4H_2O	246/40,650 305/32,786 376/26,595	π → π* n → π* MLCT	Square planner	0.0
[Pt($C_8H_{11}N_2O_3$)Cl·H_2O]2H_2O	258/38,759 305/32,786 540/18,518	π → π* n → π* 1A1g -> 1B2g	Square planner	0.0

Table 4. Thermal analyses data of the newly synthesized Ni(II)-Pd(II) and Pt(II)-chelates.

Compound	TGA. range (˚C)	% Mass loss found (calcd.)	TGA description	Residue
[Ni($C_8H_{11}N_2O_3$)Cl·H_2O]8H_2O	46.40 - 212.76 212.76 - 332.96 332.96 - 501.77	20.8 (36.8) 11.8 (15.9) 31.117 (36.02)	- the loss of 9H_2O - the loss of ethene and 1/2O_2 - the loss of CH_3Cl, NH_3 and 1/2O_2	NiO + C_5N 31.12% (36.03%)
[Pd($C_8H_{11}N_2O_3$)(CH_3COO)H_2O]4H_2O	8.80 - 250.73 251.30 -601.74	3.489 (4.1) 66.14 (71.14)	- the loss H_2O - the loss of (4H_2O, CH_3COOH and $C_8H_{11}N_2O_2$)	PdO 30.34% (27.98%)
[Pt($C_8H_{11}N_2O_3$)Cl·H_2O]2H_2O	36.56 - 279.23 279.23 -350.62 350.62 -601.43	7.75 (11.5) 7.0921 (12.4) 37.73 (41.73)	- the loss of 3H_2O - the loss of 1/2Cl_2 and 1/2O_2 - the loss of $C_8H_{11}N_2O$	PtO 47.41% (45.13%)

Table 5. Antimicrobial activity for sodium baribtone and its metal complexes (10 μg/disc for each compound).

Compound	Inhibition zone diameter (mm/mg sample)			
	Gram + bacteria *S. aureus*	Gram-bacteria *E. coli*	Fungi *C. albicans*	Fungi . .A.flavus
Sodium barbitone (ligand)	0.0	0.0	0.0	0.0
[Ni($C_8H_{11}N_2O_3$)Cl·H_2O]8H_2O	16	18	20	0.0
[Pd($C_8H_{11}N_2O_3$)(CH_3COO)H_2O]4H_2O	10	12	12	0.0
[Pt($C_8H_{11}N_2O_3$)Cl·H_2O]2H_2O	13	10	0.0	0.0

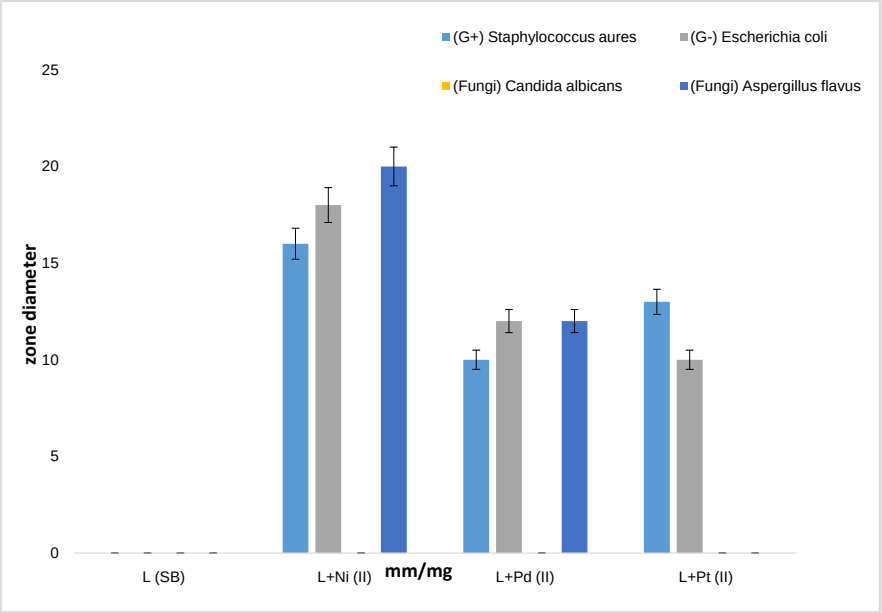

Figure 3. Biological activity of sodium barbitone and its metal complexes.

Sodium Barbitone and Its Complexes

The metal complexes biological activities (**Table 5**, **Figure 3**) are higher than the free ligand towards the gram positive, gram negative bacteria and fungi species. In case of bacteria gram positive, gram negative the Ni(II) complex show highest bacterial activity than Pd(II) and Pt(II) complexes. The antimicrobial activities of the complexes in case of *Candida albicans*, Ni(II) shows the highest fungal activity than Pd(II), but Pt(II) has no innate activity against *Candida albicans.* In case of *Aspergillus flavus* the three metals Ni(II), Pd(II) and Pt(II) complexes have no activity towards it.

The experimental data presented in **Table 5** suggest that the metal complexes of Ni(II), Pd(II) and Pt(II) are more toxic in comparison to their parent free ligand (sodium barbitone) itself in inhibiting the growth of microorganisms. This inhibiting because of the change in structure of the ligand on coordination to the metals and metal complexes when chelating act as more powerful bacteriostatic agents, so that the growth of microorganisms inhibiting. moreover, the polarity of the metal ion reduces by coordination because of the partial sharing of its positive charge with the donor groups within the chelate ring system formed during the coordination. This would suggest that the chelation could help the ability of the complex to cross a cell membrane and can be explained by Tweedy's chelation theory [25]. The Ni(II), Pd(II) and Pt(II) complexes show greater antibacterial activity towards bacteria. The variation in the activity of metal complexes against different organisms depends on the impermeability of the microorganism cells or on differences of ribosome of microbial cells [25] [26]. The increase in the antifungal activity of the metal complexes inhibits multiplication process of the microbes by blocking their activity sites. Such increased activity on metal chelation can be explained on the basis of Tweedy's chelation theory.

While chelation is not the only factor for antimicrobial activity, it is an intricate blend of several aspects such as nature of the metal ion and the ligand, the geometry of the metal complexes, the lipophilicity, steric and pharmacokinetic factors [27].

5. Conclusion

In the present study, the free ligand sodium barbitone and it corresponding group VIII metals complexes Ni(II), Pd(II) and Pt(II) were prepared and structurally identified. The structures of free ligands and its metal chelates are proved by elemental analyses and applying spectroscopic measurements (FT-IR and mass spectra) and confirmed by thermal analyses. On the basis of their analytical data, we propose square planer geometry for metal complexes. The synthesized free ligand are found to be biologically active and their metal complexes showed significantly enhanced antibacterial and antifungal activities against microbial strains in comparison to the free ligand.

Conflicts of Interest

The authors declare no conflicts of interest regarding the publication of this paper.

References

[1] Ashnagar, A., Naseri, N.G. and Sheeri, B. (2007) Novel Synthesis of Barbiturates. *Chinese Journal of Chemistry*, **25**, 382-384. https://doi.org/10.1002/cjoc.200790073

[2] Delgado, J.N., Remers, W.A. and Lippincott, J.B. (1991) Wilson and Gisvold's Textbook of Organic Medicinal Pharmaceutical Chemistry. 9th Edition, L. Williams & Wilkins, Philadelphia, 341, 376, 39.

[3] Kuhlmann, W.D. (2006) Buffer Solutions.

[4] Ruzin, S.E. (1999) Plant Microtechnique and Microscopy. Oxford University Press, Oxford.

[5] Monthony, J.F., Wallace, E.G. and Allen, D.M. (1978) A Non-Barbital Buffer for Immunoelectrophoresis and Zone Electrophoresis in Agarose Gels. *Clinical Chemistry*, **24**, 1825-1827. https://doi.org/10.1093/clinchem/24.10.1825

[6] Hueso-Urena, F., IIIan-Cabeza, N.A., Moreno-Carretero, M.N., Martinez-Martos, J.M. and Ramirez-Exposito, M.J. (2003) Synthesis and Spectroscopic Studies on the New Schiff Base Derived from the 1:2 Condensation of 2,6-Diformyl-4-methylphenol with 5-Aminouracil (BDF5AU) and Its Transition Metal Complexes: Influence on Biologically Active Peptides-Regulating Aminopeptidases. *Journal of Inorganic Biochemistry*, **94**, 326-334. https://doi.org/10.1016/S0162-0134(03)00025-4

[7] Refat, M.S., El-Korashy, S.A. and Ahmed, A.S. (2008) A Convenient Method for the Preparation of Barbituric and Thiobarbituric Acid Transition Metal Complexes. *Spectrochimica Acta A*, **71**, 1084-1094. https://doi.org/10.1016/j.saa.2008.03.001

[8] Tsunoda, A., Shibisawa, M., Yasuda, Y., Nakao, N. and Kusano, K. (1994) *Anticancer Research*, **14**, 2637-2642.

[9] Raper, E.S. (1985) Complexes of Heterocyclic Thione Donors. *Coordination Chemistry Reviews*, **61**, 115-184. https://doi.org/10.1016/0010-8545(85)80004-7

[10] Casas, J.S., Castellans, E.E., Louce, M.D., Ellena, J., Sanchez, A., Sordo, J. and Taboada, C. (2006) A Gold(I) Complex with a Vitamin K3 Derivative: Characterization and Antitumoral Activity. *Journal of Inorganic Biochemistry*, **100**, 1858-1860. https://doi.org/10.1016/j.jinorgbio.2006.07.006

[11] Campbell, M.J. (1975) Transition Metal Complexes of Thiosemicarbazide and Thiosemicarbazones. *Coordination Chemistry Reviews*, **15**, 279-319. https://doi.org/10.1016/S0010-8545(00)80276-3

[12] Rodriguez-Argüelles, M.C., Ferrari, M.B., Fava, G.G., Pelizzi, C., Tarasconi, P., Albertini, R., Dall'Aglio, P.P., Lunghi, P. and Pinelli, S. (1995) 2,6-Diacetylpyridine bis(thiosemicarbazones) Zinc Complexes: Synthesis, Structure, and Biological Activity. *Journal of Inorganic Biochemistry*, **58**, 157-175. https://doi.org/10.1016/0162-0134(94)00043-A

[13] Casas, J.S., Garcia-Tasende, M.S., Maichel-Mossmer, C., Rodriguez-Argüelles, M.C., Sanchez, A., Sordo, J., Vazquez-Lopez, A., Pinelli, S., Lunghi, P. and Albertini, R. (1996) Synthesis, Structure, and Spectroscopic Properties of Acetato (Dimethyl)(pyridine-2-carbaldehydethiosemicarbazonato)tin(IV) Acetic Acid Solvate, [$SnMe_2$(PyTSC)(OAc)].HOAc. Comparison of Its Biological Activity with That of Some Structurally Related Diorganotin(IV) Bis(thiosemicarbazonates). *Journal of Inorganic Biochemistry*, **62**, 41-55. https://doi.org/10.1016/0162-0134(95)00087-9

[14] Ferrari, M.B., Fava, G.G., Tarasconi, G., Albertini, R., Pinelli, S. and Starcich, R. (1994) Synthesis, Spectroscopic and Structural Characterization, and Biological Activity of Aquachloro(pyridoxal thiosemicarbazone) Copper(II) Chloride. *Journal of Inorganic Biochemistry*, **53**, 13-25. https://doi.org/10.1016/0162-0134(94)80017-0

[15] Koch, U., Attenni, B., Malancona, S., Colarusso, S., Conte, I., Filippo, M.D., Harper, S., Pacini, B., Giomini, C., Thomas, S., Incitti, I., Tomei, L., Francesco, R.D., Altamura, S., Matassa, V.G. and Narjes, F. (2006) 2-(2-Thienyl)-5,6-dihydroxy-4-carboxypyrimidines as Inhibitors of the Hepatitis C Virus NS5B Polymerase: Discovery, SAR, Modeling, and Mutagenesis. *Journal of Medicinal Chemistry*, **49**, 1693-1705. https://doi.org/10.1021/jm051064t

[16] Foye, W.O., Lemke, T.L. and Williams, D.A. (1995) Principles of Medicinal Chemistry. 4th Edition, Williams & Wilkins, Philadelphia, Vol. 89, 154-180.

[17] Bauer, A.W., Kirby, W.M., Sherris, C. and Turck, M. (1996) Antibiotic Susceptibility Testing by a Standardized Single Disk Method. *American Journal of Clinical Pathology*, **45**, 493. https://doi.org/10.1093/ajcp/45.4_ts.493

[18] Refat, M.S. and Sharshar, T. (2012) Infrared, Raman, 1H NMR, Thermal and Positron Annihilation Lifetime Studies of Pb(II), Sn(II), Sb(III), Bi(III)-Barbital Complexes. *Journal of Molecular Structure*, **1016**, 140-146. https://doi.org/10.1016/j.molstruc.2012.02.047

[19] Babykutty, P.V., Prabhakaran, C.P., Anantaraman, R. and Nair, C.G.R. (1974) Electronic and Infrared Spectra of Biguanide Complexes of the 3d-Transition Metals. *Journal of Inorganic and Nuclear Chemistry*, **36**, 3685-3688. https://doi.org/10.1016/0022-1902(74)80148-X

[20] Yilmaz, V.T., Aksoy, M.S. and Sahin, O. (2009) Different Coordination Modes of 5,5-Diethylbarbiturate in the Copper(II) Complexes with Some Aliphatic Amines: Synthesis, Spectroscopic, Thermal and Structural Studies. *Inorganica Chimica Acta*, **362**, 3703. https://doi.org/10.1016/j.ica.2009.04.026

[21] Timerbaev, A.R., Hartinger, C.G. and Keppler, B.K. (2006) Metallodrug Research and Analysis Using Capillary Electrophoresis. *TrAC Trends in Analytical Chemistry*, **25**, 868-875. https://doi.org/10.1016/j.trac.2006.04.009

[22] Lever, A.B.P. (1984) Inorganic Electronic Spectroscopy. 2nd Edition, Elsevier Science

Publishers, Amsterdam, 161.

[23] Sylvie, M., *et al.* (1998) Influence of Disorder on Electronic Excited States: An Experimental and Numerical Study of Alkylthiotriphenylene Columnar Phases. *The Journal of Physical Chemistry B*, **102**, 4697-4710. https://doi.org/10.1021/jp980623n

[24] Farah, M. S., Faisal, M., Nibras, M. and Shaker, C. (2016) *International Journal of Pharmaceutics*, **6**, 47-52.

[25] Tweedy, B.G. (1964) Plant Extracts with Metal Ions as Potential Antimicrobial Agents. *Phytopathology*, **55**, 910-914.

[26] Murukan, B. and Mohanan, K. (2007) Synthesis, Characterization and Antibacterial Properties of Some Trivalent Metal Complexes with [(2-hydroxy-1-naphthaldehyde)-3-isatin]-bishydrazone. *Journal of Enzyme Inhibition and Medicinal Chemistry*, **22**, 65-70. https://doi.org/10.1080/14756360601027373

[27] Thankamony, M. and Mohanan, K. (2007) *Indian Journal of Chemistry A*, **46**, 247-251.